

Analysis of NACA 0024 Airfoil Wing Calibration

Kirill Grichanichenko, Artem Grichanichenko, Maksym Shkola
Department of Physics, Edmonds Community College, Lynnwood WA 98036*
(Dated: 19 March 2024)

This research paper presents an understanding of the relationship between an experimental wing design based on the NACA 0024 airfoil and discusses testing stability by analyzing the lift-to-drag ratio. Analysis and data interpretation offer an assessment of the findings from the experimental process outlined in the following procedure section, which focuses on testing the NACA 0024 airfoil in a wind tunnel in angle increments. The dimensions of the wing are as follows: The chord length is 14cm, with a wingspan of 10cm. The maximum thickness of the wing measures 3.3cm with a total surface area of around 326.2cm^2 , and it weighs 100 grams. Testing revealed that the wing reached its maximum lift of 9.68N at an angle of 42.3° , with the highest lift-to-drag ratio recorded as 3.14N. Interestingly, at 0° , neither the experimental nor the existing dataset produced lift, with the lift-to-drag ratio at -0.42N for the experimental and 0N for the existing dataset. Both sets rapidly increased their ratios between 4° and 14.9° , with the existing dataset increasing by 7.24N per degree, while the experiment increased by 0.50N per degree. In addition, both datasets reached their peak lift-to-drag ratio within the same range of angles of attack: $6.75^\circ - 11.75^\circ$. The peak lift-to-drag ratio of the experimental data was 3.14N, while the peak lift-to-drag ratio of the existing data was 51.9N, making a 48N stability difference between the datasets. Examining the experimental data with the existing data, we can see vast differences between the two datasets. The existing dataset exhibits a 94.5% average level difference from the experimental dataset. This is due to airflow issues caused by the experimental model's testing conditions and the airfoil not being wide enough in the wind tunnel, which caused air to slip off the sides of the wing, resulting in airflow issues. However, it is important to note that even with the differences, the experimental data still follows the fundamental patterns seen in the existing data. While the experimental data strays from the 95% confidence interval, when explained in the context of our experimental setup and the consistency of the experimental data following the existing data's patterns, it shows us an accurate representation of the NACA 0024 airfoil wing design and flight stability.

Keywords: PHYS 222; drag; lift; thrust; gravity; Bernoulli's equation; airfoil; wing;

I. INTRODUCTION

Many people have been in an airplane at some point in their lives. But still, it is often the case that understanding flight remains a mystery. How does it fly? What is the purpose of the wings, and why are they designed the way they are? Comprehending aerodynamic flight is an important principle for understanding airplanes.

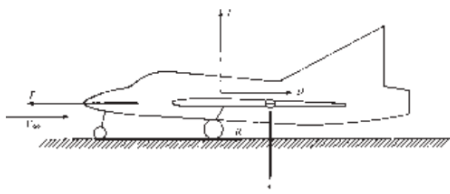


FIG. 1. Forces acting on an airplane

A. Basic Terminology

Firstly, to understand the aerodynamics of airplanes, we must first define some terms used throughout the paper. To begin, we will use the term aircraft throughout the paper as a reference to airplanes. Aircraft have four main components influencing their motion through the air, aka flight. The first of the four components is thrust. Thrust in an aircraft is the force that gives the aircraft its movement, or, in other words, it is the force that propels the aircraft to achieve the speed needed to get into the air. Some examples of thrust would be the engine on a plane propelling it forward or the force generated by the throwing motion in the case of a paper airplane. The second of the four components is lift. Lift on an aircraft is the primary force that enables the aircraft to move up against gravity and is mostly generated through the wings of the aircraft. The construction of the wings plays a crucial role in creating lift. The third of the four components is gravity. Gravity is the vertical downward force upon the aircraft that pulls the aircraft toward the Earth. Gravity and lift combat each other and must be in equilibrium for flight.

* Emails:

kirillkongrichanichenko@gmail.com,
ArtemGrichanichenko@gmail.com,
maksymvshkola@gmail.com

¹ Graphical elements in this paper have been taken from Anderson and Glenn Research Center, et. al.,[11],[7]. Photographs are by the author.

Lastly, the fourth of the four components is drag. Drag is the force that the aircraft experiences when it is in motion, and it is the air molecules pulling the aircraft in the opposite direction of the aircraft's flight path. In most cases, reducing the drag of the aircraft improves the aircraft's flight performance. Another term is Newton's first law, which states: "An object at rest remains at rest, and an object in motion remains in motion at a constant speed and in a straight line unless acted on by an unbalanced force." [7] Newton's first law is closely related to the aircraft's thrust, which gets the aircraft in motion. In addition to Newton's first law, Newton's third law, combined with the Coanda effect and Bernoulli's principle, plays a critical role in explaining how the wing of an aircraft generates lift. Newton's third law states: "Whenever one object exerts a force on another object, the second object exerts an equal and opposite force on the first." [7] The Coanda Effect is "the phenomenon in which a jet flow attaches itself to a nearby surface and remains attached even when the surface curves away from the initial jet direction." [8] Meaning, that airflow will follow the shape of whatever it encounters. Bernoulli's principle states that "an increase in the speed of a fluid occurs simultaneously with a decrease in pressure or a decrease in the fluid's potential energy" [9]. Meaning, that air moving faster and at a greater distance has less pressure than air moving slower but at a shorter distance. Refer to sub-topic C: Role of Wings, to fully understand how these principles work together to generate lift.

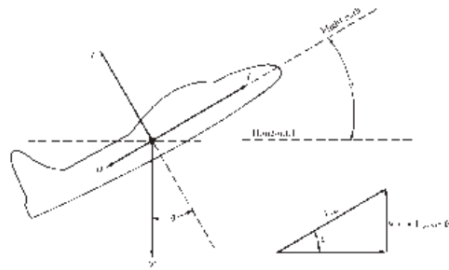


FIG. 2. Airplane in climbing flight

B. General Motion Of An Aircraft In The Air/Aerodynamics

The general motion of an aircraft in the air is tied to the four main forces that act upon the aircraft: lift, drag, thrust, and gravity. Manipulating these forces to be relatively equal to each other initiates flight. In addition, understanding how to assess these forces allows for the measurement and interpretation of the efficiency, stability, and overall performance of the aircraft. Before an aircraft takes flight, drag needs to be respected, and if an aircraft does not consider the drag, the whole goal of flight will not be possible. The friction between air molecules and the aircraft causes drag during flight, which prevents the aircraft from moving forward. Hence,

the need for aerodynamic design of aircraft and wings. The design of the aircraft and wings combat drag by creating arrow-like configurations that allow air fluids to pass by the aircraft with less friction, which minimizes drag. The flight process can begin once drag has been taken into account. When an aircraft is about to get into the air, it needs a powerful force to push it forward and give it speed for takeoff; this is where thrust is introduced. The idea of thrust is derived from Newton's first law and is the external force that propels the aircraft to move forward. During model aircraft testing, thrust can be substituted for the aircraft's engines using other forces. While thrust is an important factor for flight, it is still not enough to get the aircraft into the air. When an aircraft is about to take flight, it experiences another external force acting on it that keeps it from flying, called gravity. Gravity is the force that acts upon the aircraft's weight and pulls it toward Earth. At first glance, gravity might seem like the main force that needs to be countered for flight, and a common thought is to get rid of gravity, and you will achieve flight. However, it is important to recognize the usefulness of gravity because carefully managing gravity allows for controlled ascent and descent without using more than needed external thrust, which improves fuel efficiency. Now, acknowledging drag, thrust, and gravity introduces the final force, lift. The previous forces all acted in the forward, backward, and downward directions, but the lift is responsible for the upward direction of the aircraft. Lift is primarily established by the wings of an aircraft and is used to balance out gravity to generate flight. Lift is created when air molecules hit the wings at a certain point, which causes the air molecules to push the aircraft upward. More will be explained in sub-topic C: Role of Wings.

Moving on, considering all four forces and carefully controlling them, we can establish flight. In a general flight operation, this is how these forces will interact with each other during different phases of flight. At first, during takeoff, thrust is increased to overcome gravity's pull on the weight of the aircraft, and as the aircraft speeds up, the lift is generated through the wings of the aircraft, slowly increasing its lift over the weight. At a certain point, the lift will overcome the weight, allowing the aircraft to lift off the ground. After takeoff, the aircraft will start its ascent, continue to use thrust, and increase its lift over the weight to reach a certain altitude. When the preferred altitude is reached, the aircraft stops using thrust and instead relies on drag to keep the aircraft in a steady state where thrust equals drag and lift equals weight. In addition, it is at this point that flight stability is measured by calculating the lift-to-drag ratio. When an aircraft is ready to land, it utilizes gravity and begins its descent by decreasing thrust until its weight exceeds lift. At the landing phase, the thrust is decreased while the lift is increased to achieve a soft landing.

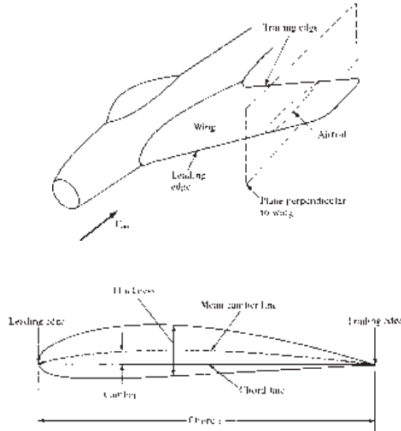


FIG. 3. Sketch of wing and airfoil

C. Role of Wings

The wings of an aircraft are crucial in aerodynamics and are essential in allowing the aircraft to achieve flight. The general role of the wing is to produce lift, and the way a wing produces lift is through four main components: airfoil shape, angle of attack, wing area, and airflow. Furthermore, many other components influence how a wing produces lift, but due to time constraints and the purpose of the experiment, only these four will be discussed. First off, the airfoil shape of the wing was created to exploit Bernoulli's principle. It is designed by making the top of the wing look like a stretched-out half-oval and the lower part of the wing more relatively flat. This is done so that when air molecules hit the wing of the aircraft, some air goes over the top of the wing and some goes over the bottom, splitting the airflow. When the airflow splits due to the design of the wing, the air on top of the wing travels longer and faster, which causes it to have less pressure than the air at the bottom, which travels slower. This variation in airspeed creates a pressure difference on the wing, resulting in an upward force known as lift. Secondly, there is the angle of attack. The angle of attack of a wing is the angle at which the wing meets the oncoming air, and adjusting the angle of attack can affect how much lift is generated or lost. In addition, the angle of attack has boundaries, and too much angle of attack can cause the airflow to become unstable, and lift could decrease.

The next component is airflow. The airflow of the wing is how the air moves about the wing, which is usually connected to the Coanda effect. The Coanda effect reveals Newton's third law and shows that when air goes around a wing, the air going on top of the wing leaves the wing by pushing the back of the wing downwards, which then pushes the top of the wing upwards, causing lift. Airspeed also connects with the airflow of the wing, and the speed at which the aircraft moves directly affects how much lift gets generated due to how aggressively the air leaves the wing. Lastly, there is the wing area and

size of the overall wing. The area of a wing is a principal factor to consider when talking about a wing's lift performance, and that is because the amount of wing area directly affects how much space there is for air to interact with the wing. In addition, this also directly influences all the other components that affect how a wing generates lift. Taking all those factors together shows the purpose of an aircraft's wings. Sub-topic D: Wing Geometry, will explain in more detail the key design of our airfoil wing that will be tested.

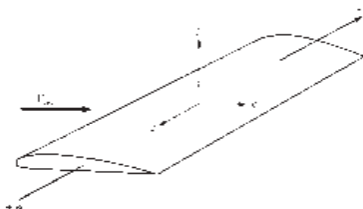


FIG. 4. Airfoil wing

D. Wing Geometry

Following our discussion of wing principles, we will move on to our main experimental wing airfoil design, and how we created it. The experimental wing design includes a symmetrical top and bottom airfoil shape with a straight leading edge. The airfoil has a curved upper surface that is mirrored with the lower surface and reaches its maximum thickness of 24% of the chord length, and this maximum thickness is located at 30% of the chord length measured from the leading edge. Since the airfoil is symmetric there is no camber at the leading edge so 0% chord, and the camber gradually decreases symmetrically along the chord length. This design was inspired by the NACA 0024 airfoil wing design which was developed by the National Advisory Committee for Aeronautics. This design allows us to minimize any wandering variables and allows us to produce an efficient and working wing to be tested and compared with ongoing data. In terms of measurements of the wing, the chord length is 14cm, with a wingspan of 10cm. The max thickness of the wing measures 3.3cm with a total surface area of around 326.2cm^2 . This aircraft airfoil was created with the intent to be able to fit into the testing area, so full-scale measurements might be off by a slight margin. The experimental wing was 3D printed using an STL file for testing model aircraft wings. Refer to [14] to find the STL file used for this experiment. Overall, this explains our experimental wing design.

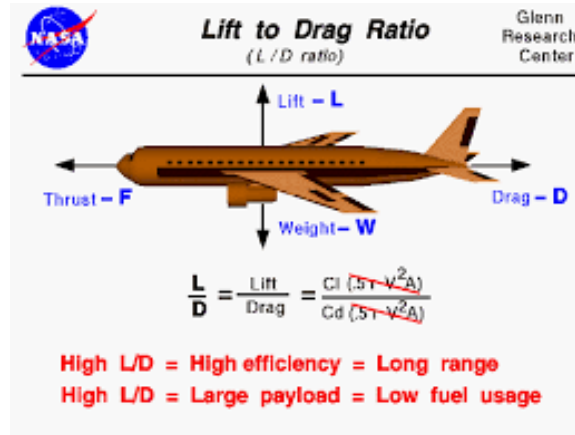


FIG. 5. Lift-To-Drag Ratio

E. Testing Stability With Lift-To-Drag Ratio

Now that we have covered how an aircraft works, the role of wings, and our experimental wing design, we need to explain our testing procedure. For this specific experiment, we will focus on the stability and effectiveness of an aircraft calculated through its lift-to-drag ratio, but before we get into the lift-to-drag ratio, we need to explain what the stability of an aircraft is. The stability of an aircraft is a major aspect that engineers look for in an aircraft, as it directly influences the safety, performance, and overall operability of the aircraft. The stability of an aircraft is the measurement of how effectively the aircraft can maintain a constant flight attitude and recover if it has been intentionally or unintentionally disturbed from its flight path. A common and one of the most effective ways of measuring an aircraft's stability is through the lift-to-drag ratio. The lift-to-drag ratio is a parameter that shows how effective an aircraft is in generating lift compared to the drag it experiences during flight. In addition, since lift is primarily generated in the wings of an aircraft, this would be a perfect metric to measure the stability of an aircraft while testing the wing airfoil. To measure the lift-to-drag ratio in our experiment, we will test our wing airfoil in a wind tunnel located at Monroe Hall in Edmonds College. We will experiment with our NACA 0024 wing airfoil (as discussed in sub-topic D: Wing Geometry) and change between angles of attack; starting with 0° and increasing the angle by one unit until we reach a stall by the airfoil. During the experiment, we will control the following aspects: airspeed, yaw angle, wing design, etc, while only manipulating the angle of attack. After every angle, we will record the lift generated by the aircraft and the drag it experiences during testing. To record the lift and drag of the aircraft, we will use a force balance tool that allows for the measurements of forces like lift and drag, and after that, we will divide the lift by the drag (lift/drag) to get our lift-to-drag ratio. In the end, this metric will serve as a key indicator of stability and how well the airfoil wing per-

formed at different angles of attack. Higher values of the lift-to-drag ratio will indicate a more efficient and stable flight. In addition, to our experimental data, we also want to compare our data with available datasets on the NACA 0024 airfoil wing to help us understand how well our airfoil did compared to higher-end existing data sets and explain any differences and similarities that we come across. This will help us further understand where the NACA 0024 airfoil wing has its strengths and weakness.

II. EXPERIMENT

A. Materials and Apparatus

1. Materials

1. TPU plastic filament: is the main material used to construct the airfoil wing.
2. Metal stud testing rod (1/4-20): This was used to place and hold the airfoil wing in the wind tunnel.
3. Wind Tunnel (Monroe Hall, Edmonds College): The wind tunnel at Monroe Hall, Edmonds College, was used to evaluate the aerodynamic properties of the airfoil.

2. Apparatus

The apparatus is a NACA 0024 Airfoil that was 3D printed using blue TPU plastic filament. To construct this experiment there was a wide range of machinery, software, and materials used. Solid works computer software was used to design the apparatus ensuring the proper dimensions, weight, and aerodynamics. Once the design was complete, a 3D printer with TPU plastic filament 3d printed the design. The dimensions are L: 14cm, W: 10cm, Height/Thickness: 3.3cm and the weight is 100 grams.

B. Procedure

To get our airfoil, we used a 3D printer to print the airfoil and used a wind tunnel to test the airfoil for the lift-to-drag ratio. Since the airfoil has a symmetric design, it did not matter whether we placed it upright or upside down.

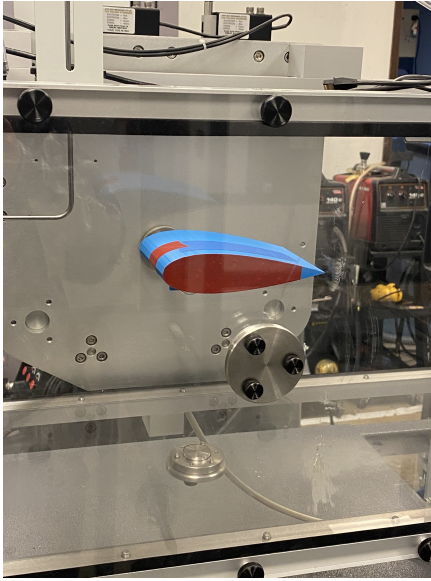


FIG. 6. Experimental airfoil in wind tunnel



FIG. 8. Tool used to manipulate the angle of attack

During our 1st test, we used a wind speed of 18.50m/s , and every time we increased the angle by 1° starting at 0° to 30° . We decided to do another test at a higher wind speed of 28.50m/s and increase the angle by 1° starting at 0° to 48° .



FIG. 7. Wind tunnel used during experiment

After completing both tests, we did a final test without the airfoil and just the rod to get the rod's lift and drag to subtract it from the combined lift and drag of the airfoil with the rod. After collecting all the needed data, the wind tunnel operator sent us all the data recorded via an Excel sheet, which we later used to analyze and conclude our research.

III. DATA AND ANALYSIS

After finishing the experiment with the NACA airfoil wing, we had a large amount of raw data, and in this section, we want to walk through the process of analyzing that data. To start, after finishing our experiment using the wind tunnel, we were left with the following data: Refer to Figures 9

Run Number	Angle of Attack	Drag (N)	Pitching Moment (N-m)	Mass of Airfoil (kg)	Wind Speed (m/s)	CFD Input (m/s)	Gravitational Constant (m/s)	Operating Conditions (Temperature °C)	Atmospheric Pressure (Pa)	Ambient Air Density (kg/m³)	Calibrated Windspeed (m/s)
1	0.00	-0.00	-0.00	0.00	18.50	18.50	9.81	-	101320	1.225	18.50
2	0.00	-0.00	-0.00	0.00	18.50	18.50	9.81	-	101320	1.225	18.50
3	0.00	-0.00	-0.00	0.00	18.50	18.50	9.81	-	101320	1.225	18.50
4	0.00	-0.00	-0.00	0.00	18.50	18.50	9.81	-	101320	1.225	18.50
5	0.00	-0.00	-0.00	0.00	18.50	18.50	9.81	-	101320	1.225	18.50
6	0.00	-0.00	-0.00	0.00	18.50	18.50	9.81	-	101320	1.225	18.50
7	0.00	-0.00	-0.00	0.00	18.50	18.50	9.81	-	101320	1.225	18.50
8	0.00	-0.00	-0.00	0.00	18.50	18.50	9.81	-	101320	1.225	18.50
9	0.00	-0.00	-0.00	0.00	18.50	18.50	9.81	-	101320	1.225	18.50
10	0.00	-0.00	-0.00	0.00	18.50	18.50	9.81	-	101320	1.225	18.50
11	0.00	-0.00	-0.00	0.00	18.50	18.50	9.81	-	101320	1.225	18.50
12	0.00	-0.00	-0.00	0.00	18.50	18.50	9.81	-	101320	1.225	18.50
13	0.00	-0.00	-0.00	0.00	18.50	18.50	9.81	-	101320	1.225	18.50
14	0.00	-0.00	-0.00	0.00	18.50	18.50	9.81	-	101320	1.225	18.50
15	0.00	-0.00	-0.00	0.00	18.50	18.50	9.81	-	101320	1.225	18.50
16	0.00	-0.00	-0.00	0.00	18.50	18.50	9.81	-	101320	1.225	18.50
17	0.00	-0.00	-0.00	0.00	18.50	18.50	9.81	-	101320	1.225	18.50
18	0.00	-0.00	-0.00	0.00	18.50	18.50	9.81	-	101320	1.225	18.50
19	0.00	-0.00	-0.00	0.00	18.50	18.50	9.81	-	101320	1.225	18.50
20	0.00	-0.00	-0.00	0.00	18.50	18.50	9.81	-	101320	1.225	18.50
21	0.00	-0.00	-0.00	0.00	18.50	18.50	9.81	-	101320	1.225	18.50
22	0.00	-0.00	-0.00	0.00	18.50	18.50	9.81	-	101320	1.225	18.50
23	0.00	-0.00	-0.00	0.00	18.50	18.50	9.81	-	101320	1.225	18.50
24	0.00	-0.00	-0.00	0.00	18.50	18.50	9.81	-	101320	1.225	18.50
25	0.00	-0.00	-0.00	0.00	18.50	18.50	9.81	-	101320	1.225	18.50
26	0.00	-0.00	-0.00	0.00	18.50	18.50	9.81	-	101320	1.225	18.50
27	0.00	-0.00	-0.00	0.00	18.50	18.50	9.81	-	101320	1.225	18.50
28	0.00	-0.00	-0.00	0.00	18.50	18.50	9.81	-	101320	1.225	18.50
29	0.00	-0.00	-0.00	0.00	18.50	18.50	9.81	-	101320	1.225	18.50
30	0.00	-0.00	-0.00	0.00	18.50	18.50	9.81	-	101320	1.225	18.50
31	0.00	-0.00	-0.00	0.00	18.50	18.50	9.81	-	101320	1.225	18.50
32	0.00	-0.00	-0.00	0.00	18.50	18.50	9.81	-	101320	1.225	18.50
33	0.00	-0.00	-0.00	0.00	18.50	18.50	9.81	-	101320	1.225	18.50
34	0.00	-0.00	-0.00	0.00	18.50	18.50	9.81	-	101320	1.225	18.50
35	0.00	-0.00	-0.00	0.00	18.50	18.50	9.81	-	101320	1.225	18.50
36	0.00	-0.00	-0.00	0.00	18.50	18.50	9.81	-	101320	1.225	18.50
37	0.00	-0.00	-0.00	0.00	18.50	18.50	9.81	-	101320	1.225	18.50
38	0.00	-0.00	-0.00	0.00	18.50	18.50	9.81	-	101320	1.225	18.50
39	0.00	-0.00	-0.00	0.00	18.50	18.50	9.81	-	101320	1.225	18.50
40	0.00	-0.00	-0.00	0.00	18.50	18.50	9.81	-	101320	1.225	18.50
41	0.00	-0.00	-0.00	0.00	18.50	18.50	9.81	-	101320	1.225	18.50
42	0.00	-0.00	-0.00	0.00	18.50	18.50	9.81	-	101320	1.225	18.50
43	0.00	-0.00	-0.00	0.00	18.50	18.50	9.81	-	101320	1.225	18.50
44	0.00	-0.00	-0.00	0.00	18.50	18.50	9.81	-	101320	1.225	18.50
45	0.00	-0.00	-0.00	0.00	18.50	18.50	9.81	-	101320	1.225	18.50
46	0.00	-0.00	-0.00	0.00	18.50	18.50	9.81	-	101320	1.225	18.50
47	0.00	-0.00	-0.00	0.00	18.50	18.50	9.81	-	101320	1.225	18.50
48	0.00	-0.00	-0.00	0.00	18.50	18.50	9.81	-	101320	1.225	18.50
49	0.00	-0.00	-0.00	0.00	18.50	18.50	9.81	-	101320	1.225	18.50
50	0.00	-0.00	-0.00	0.00	18.50	18.50	9.81	-	101320	1.225	18.50
51	0.00	-0.00	-0.00	0.00	18.50	18.50	9.81	-	101320	1.225	18.50
52	0.00	-0.00	-0.00	0.00	18.50	18.50	9.81	-	101320	1.225	18.50
53	0.00	-0.00	-0.00	0.00	18.50	18.50	9.81	-	101320	1.225	18.50
54	0.00	-0.00	-0.00	0.00	18.50	18.50	9.81	-	101320	1.225	18.50
55	0.00	-0.00	-0.00	0.00	18.50	18.50	9.81	-	101320	1.225	18.50
56	0.00	-0.00	-0.00	0.00	18.50	18.50	9.81	-	101320	1.225	18.50
57	0.00	-0.00	-0.00	0.00	18.50	18.50	9.81	-	101320	1.225	18.50
58	0.00	-0.00	-0.00	0.00	18.50	18.50	9.81	-	101320	1.225	18.50
59	0.00	-0.00	-0.00	0.00	18.50	18.50	9.81	-	101320	1.225	18.50
60	0.00	-0.00	-0.00	0.00	18.50	18.50	9.81	-	101320	1.225	18.50
61	0.00	-0.00	-0.00	0.00	18.50	18.50	9.81	-	101320	1.225	18.50
62	0.00	-0.00	-0.00	0.00	18.50	18.50	9.81	-	101320	1.225	18.50
63	0.00	-0.00	-0.00	0.00	18.50	18.50	9.81	-	101320	1.225	18.50
64	0.00	-0.00	-0.00	0.00	18.50	18.50	9.81	-	101320	1.225	18.50
65	0.00	-0.00	-0.00	0.00	18.50	18.50	9.81	-	101320	1.225	18.50
66	0.00	-0.00	-0.00	0.00	18.50	18.50	9.81	-	101320	1.225	18.50
67	0.00	-0.00	-0.00	0.00	18.50	18.50	9.81	-	101320	1.225	18.50
68	0.00	-0.00	-0.00	0.00	18.50	18.50	9.81	-	101320	1.225	18.50
69	0.00	-0.00	-0.00	0.00	18.50	18.50	9.81	-	101320	1.225	18.50
70	0.00	-0.00	-0.00	0.00	18.50	18.50	9.81	-	101320	1.225	18.50
71	0.00	-0.00	-0.00	0.00	18.50	18.50	9.81	-	101320	1.225	18.50
72	0.00	-0.00	-0.00	0.00	18.50	18.50	9.81	-	101320	1.225	18.50
73	0.00	-0.00	-0.00	0.00	18.50	18.50	9.81	-	101320	1.225	18.50
74	0.00	-0.00	-0.00	0.00	18.50	18.50	9.81	-	101320	1.225	18.50
75	0.00	-0.00	-0.00	0.00	18.50	18.50	9.81	-	101320	1.225	18.50
76	0.00	-0.00	-0.00	0.00	18.50	18.50	9.81	-	101320	1.225	18.50
77	0.00	-0.00	-0.00	0.00	18.50	18.50	9.81	-	101320	1.225	18.50
78	0.00	-0.00	-0.00	0.00	18.50	18.50	9.81	-	101320	1.225	18.50
79	0.00	-0.00	-0.00	0.00	18.50	18.50	9.81	-	101320	1.225	18.50
80	0.00	-0.00	-0.00	0.00	18.50	18.50	9.81	-	101320	1.225	18.50
81	0.00	-0.00	-0.00	0.00	18.50	18.50	9.81	-	101320	1.225	18.50
82	0.00	-0.00	-0.00	0.00	18.50	18.50	9.81	-	101320	1.225	18.50
83	0.00	-0.00	-0.00	0.00	18.50	18.50	9.81	-	101320	1.225	18.50
84	0.00	-0.00	-0.00	0.00	18.50	18.50	9.81	-	101320	1.225	18.50
85	0.00	-0.00	-0.00	0.00	18.50	18.50	9.81	-	101320	1.225	18.50
86	0.00	-0.00	-0.00	0.00	18.50	18.50	9.81	-	101320	1.225	18.50
87	0.00	-0.00	-0.00	0.00	18.50	18.50	9.81	-	101320	1.225	18.50
88	0.00	-0.00	-0.00	0.00	18.50	18.50	9.81	-	101320	1.225	18.50
89	0.00	-0.00	-0.00	0.00	18.50	18.50	9.81	-	101320	1.225	18.50
90	0.00	-0.00	-0.00	0.00	18.50						

and using what we have explained, we could condense the data further into a more understandable format, where the lift and drag could be seen at different angles of attack. Refer to FIG. 10.

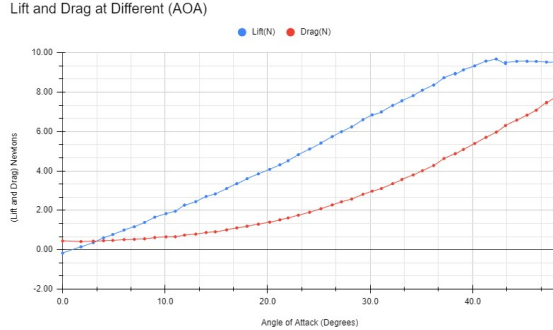


FIG. 10. Lift and Drag at different (AOA)

This graph reveals the overall flight of the wing, with the wind speed kept controlled at a relatively constant 28.50m/s and the air density also maintained at 1.17kg/m^3 . As we can see, the flight of the aircraft is good, and the data shows that our experimental wing airfoil produces enough lift to allow the aircraft to be airborne, a positive indicator that the airfoil works.

At the start, when the angle of attack was at 0° , the airfoil was not producing any lift -0.18N but was instead overcome by drag 0.43N . This is an interesting observation as we expected the airfoil to be able to produce enough lift to take flight at 0° . We suspect that the reason the airfoil does not produce lift at 0° is due to the airfoil's symmetrical design, which doesn't give the air the split it needs to counterbalance the air pressures in the wing to achieve lift at 0° . However, once the angle begins to increase, we can see a positive increase in the lift, and at 4° , we can see the lift of 0.61N overtake the drag of 0.45N , and the wing becomes airborne.

Surpassing 4° , we can see that as the angle increases, the lift of the wing also increases linearly, and between angles 4° and 42.3° , the flight stability of the aircraft is good, and the wing is producing lift at a constant rate. Nevertheless, the wing reaches its maximum lift of 9.68N at an angle of 42.3° and starts its decline. From that point, if the angle were to increase further, the drag would eventually overtake the lift, and the wing would experience a stall.

Moving on, to condense this data further, we will now evaluate the lift-to-drag ratio produced at each angle by dividing the lift by the drag. This will help us better understand the flight stability of the wing. Refer to Figure 11.

Now that we have evaluated the lift-to-drag ratio produced at each angle, we can see, in more detail, the airfoil's overall flight stability throughout the experiment. As you can see, the flight stability of the aircraft is low at 0° and produces a lift-to-drag ratio of -0.42N , but this is expected as the airfoil was not producing any lift at

Lift-To-Drag at Different (AOA)

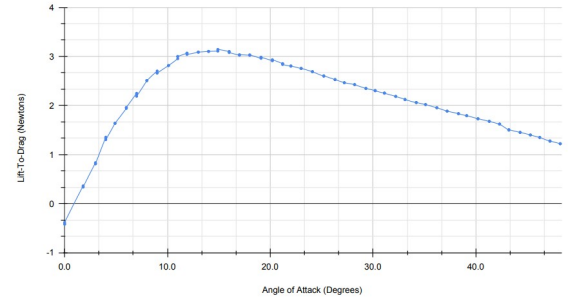


FIG. 11. Lift-To-Drag at different (AOA)

0° . Once the angle began to increase, the lift-to-drag ratio increased. Between angles 4° and 14.9° , we saw a rapid increase in the lift-to-drag ratio, marking the angle area at which flight stability of the airfoil was at its best with its peak hitting a lift-to-drag ratio of 3.14N . However, increasing the angle past 14.9° , we see a decline in the airfoil's lift-to-drag ratio, telling us that the flight stability of the aircraft declines past the angle of 14.9° . Another interesting observation happened around angles 10° and 20° , we see some small fluctuations in the data points, telling us that the airfoil started to experience some turbulence in that area.

Moving forward, this graph is still missing a key element: a comparison with existing datasets. As explained in sub-topic E: Testing Stability With Lift-To-Drag Ratio, we plan on comparing our data with existing datasets to understand how well our airfoil did compared to higher-end existing data sets and explain any differences and similarities that we come across. To accomplish this, we will extract datasets from the NACA airfoil database search (Aerospace Engineering, 2022), convert the data to obtain lift-to-drag ratios, and then graph both our experimental data and the existing dataset. Through this, we get the following data. Refer to Figure 12.

Lift-To-Drag at Different (AOA)

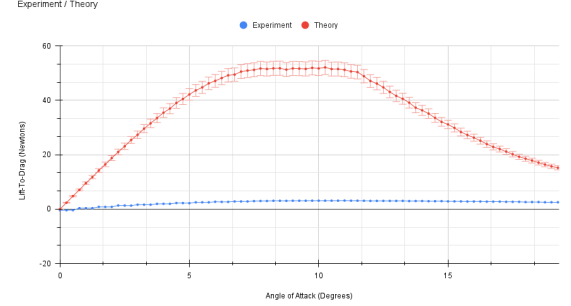


FIG. 12. Lift-To-Drag at different (AOA) compared with existing data

Examining the experimental data with existing data, we can see vast differences between the two datasets. The

existing data set exhibits a 94.5% average level difference from the experimental data set. However, we can see that the existing data has a distinct pattern that the experimental data slightly follows, indicating that the experimental data is still on track. We can observe how both data sets share a common similarity at an angle of 0°, and neither produces sufficient lift. The lift-to-drag ratio of the experimental data was recorded at -0.42N, while the lift-to-drag ratio of the existing data was 0N. Another similarity occurs when both data sets start increasing the angle of attack and begin producing lift. Climbing to their max lift-to-drag ratios, both data sets rapidly increased between angles 0° - 6.75°, where the existing data was producing a lift-to-drag ratio of 7.24N per one-angle increase, and the experimental data was producing a lift-to-drag ratio of 0.50N per one-angle increase. In addition, both data sets reached their peak lift-to-drag ratios within the same angles of attack 6.75° - 11.75°. The peak lift-to-drag ratio of the experimental data was 3.14N, while the peak lift-to-drag ratio of the existing data was 51.9N, making a 48.8N stability difference between the data sets.

Now, let's discuss why there are such drastic differences between the two datasets. As mentioned before, the existing data is at a 94.5% average level difference from the experimental data, meaning that, on average, the lift-to-drag ratios in the existing data are 94.5% greater than the lift-to-drag ratios in the experimental data. This tells us that the existing data is producing a more stable and efficient flight compared to the experimental data. This difference between the two datasets comes from the testing conditions of the experimental model airfoil. During the testing of the airfoil, the wing was not wide enough in the testing area of the wind tunnel, causing the wing to not fully capture the oncoming airflow over its entire wing span. When an airfoil is not wide enough in the wind tunnel, it causes air to slip off the sides of the wing, resulting in issues in the airflow. As a result, this directly affects the lift and drag measurements. In addition, the differences between the datasets are also due to the experimental airfoil not being exactly like the airfoil used in the theory data. Despite all this, it is important to note that even with the differences, the experimental data still follows the fundamental patterns seen in the existing data. While the experimental data strays from the 95% confidence interval, when explained in the context of our experimental setup and the consistency of the experimental data following the existing data's patterns, it shows us an accurate representation of the NACA 0024 airfoil wing design and flight stability.

IV. CONCLUSION

After analyzing and comparing our data with the existing NACA 0024 airfoil data, we discovered the relationship between the angle of attack and the lift-to-drag ratio generated by the airfoil. Comparing our experimen-

tal data with existing datasets revealed significant differences and similarities between the two datasets. Neither dataset produced sufficient lift at an angle of 0°, only generating a lift-to-drag ratio of -0.42N, which relates to the existing data that produces a lift-to-drag ratio of 0N. In the experimental dataset, we observed a steady increase in the lift at 4°, resulting in a lift-to-drag of 1.36N, whereas the existing dataset exhibited a steady increase in the lift as soon as it increased from 0°, producing a lift-to-drag ratio of 2.37N. Both datasets increased rapidly; the experimental data produced a lift-to-drag ratio of 0.50N per one-angle increase, while the theoretical data produced a lift-to-drag ratio of 7.24N per one-angle increase, resulting in a 6.74N per one-angle increase difference between the datasets. Both datasets reached their peak lift-to-drag ratio between the same angles of attack; the experimental lift-to-drag ratio of 3.14N and the existing lift-to-drag ratio of 51.9N resulted in a 48.8N stability difference. As we approached extreme angles of attack, we encountered some challenges in both datasets where the lift-to-drag ratio declined due to stall. Addressing the differences in the datasets, the main factor for the differences between the two datasets was the narrow width of the experimental airfoil in the wind tunnel testing area. The narrow width of the airfoil held it back from capturing the incoming airflow effectively across its entire span, resulting in airflow slipping off the wing's sides and disrupting airflow. However, even with these differences, it is essential to recognize the similar fundamental patterns between the experimental and existing datasets. For further research, we will address the issues in the size of the airfoil with the dimensions of the wind tunnel to remove any airflow inconsistencies.

V. FUTURE WORK

For future research, we plan to develop an improved wing using the NACA 0024 airfoil as a model. We'll start by creating a hole in the middle of the airfoil to place the rod where the center mass would be, and expanding the airfoil width so the airflow will not slip off the sides of the wings and disrupt airflow, which might help us get within the 95% confidence interval. Then, we will test our new wing in the wind tunnel twice, keeping the same wind speed in both trials to get the most accurate data possible and compare the lift-drag ratio to the original wing's lift-drag ratio to see which one performs better.

ACKNOWLEDGMENTS

We would like to thank Tom Fleming EdCC for the helpful resources, the wind tunnel operators, William Hamp and Nicole Giovine for operating the wind tunnel and providing the results of the tests, and Aigerim Rakhat for 3D printing the NACA 0024 Airfoil Wing for us.

Appendix A: LIFT, DRAG, AND MOMENT COEFFICIENTS

Again appealing to intuition, we note that it makes sense that for an airplane in flight, the actual magnitudes of L , D , and M depend not only on α but also on velocity and altitude. In fact, we can expect that the variations of L , D , and M depend at least on:

1. Free-stream velocity V_∞ .
2. Free-stream density ρ_∞ (that is, altitude).
3. Size of the aerodynamic surface. For airplanes, we will use the wing area S to indicate size.
4. Angle of attack α .
5. Shape of the airfoil.
6. Viscosity coefficient μ_∞ (because the aerodynamic forces are generated in part from skin friction distributions).
7. Compressibility of the airflow. In Chapter 4, we demonstrated that compressibility effects are governed by the value of the free-stream Mach number $M_\infty = V_\infty/a_\infty$. Because V_∞ is already listed, we can designate a_∞ as our index for compressibility.

Hence, we can write that for a given shape of airfoil at a given angle of attack:

$$L = f(V_\infty, \rho_\infty, S, \mu_\infty, a_\infty). \quad (\text{A1})$$

and D and M are similar functions.

In principle, for a given airfoil at a given angle of attack, we could find the variation of L by performing myriad wind tunnel experiments wherein V_∞ , ρ_∞ , S , μ_∞ , and a_∞ are individually varied, and then we could try to make sense out of the resulting huge collection of data. This is the hard way. Instead, we ask: Are there groupings of the quantities V_∞ , ρ_∞ , S , μ_∞ , a_∞ , and L such that Equation (1) can be written in terms of fewer parameters? The answer is yes. In the process of developing this answer, we will gain some insight into the beauty of nature as applied to aerodynamics.

The technique we will apply is a simple example of a more general theoretical approach called dimensional analysis. Let us assume that Equation (1) is of the functional form:

$$L = ZV_\infty^a \rho_\infty^b S^d \alpha_\infty^e \mu_\infty^f, \quad (\text{A2})$$

where Z , a , b , d , e , and f are dimensionless constants. However, no matter what the values of these constants may be, it is a physical fact that the dimensions of the left and right sides of Equation (2) must match; that is, if L is a force (say in newtons), then the net result of all the exponents and multiplication on the right side must also produce a result with the dimensions of a force. This

constraint will ultimately give us information about the values of a , b , and d .

If we designate the basic dimensions of mass, length, and time by m , l , and t , respectively, then the dimensions of various physical quantities are as given in the following:

$$\begin{aligned} L &= \frac{ml}{t^2} \quad (\text{from Newton's second law}) \\ V_\infty &= \frac{l}{t} \\ \rho_\infty &= \frac{m}{l^3} \\ S &= l^2 \\ a_\infty &= \frac{l}{t} \\ \mu_\infty &= \frac{m}{lt}. \end{aligned}$$

Thus equating the dimensions of the left and right sides of Equation (2), we obtain:

$$\frac{ml}{t^2} = \left(\frac{l}{t}\right)^a \left(\frac{m}{l^3}\right)^b (l^2)^d \left(\frac{l}{t}\right)^e \left(\frac{m}{lt}\right)^f. \quad (\text{A3})$$

Consider mass m . The exponent of m on the left side is 1, so the exponents of m on the right must add to 1. Hence:

$$1 = b + f. \quad (\text{A4})$$

Similarly, for time t we have:

$$-2 = -a - e - f. \quad (\text{A5})$$

And for length l :

$$1 = a - 3b + 2d + e - f. \quad (\text{A6})$$

Solving Equations (4) to (6) for a , b , and d in terms of e and f yields:

$$b = 1 - f, \quad (\text{A7})$$

$$a = 2 - e - f, \quad (\text{A8})$$

$$d = 1 - \frac{f}{2}. \quad (\text{A9})$$

Substituting Equations (8) to (9) into Equation (2) gives:

$$L = ZV_\infty^{2-e-f} \rho_\infty^{1-f} S^{1-\frac{f}{2}} \alpha_\infty^e \mu_\infty^f. \quad (\text{A10})$$

Rearranging Equation (10), we find:

$$L = Zp_\infty V_\infty^2 S \left(\frac{\alpha_\infty}{v_\infty}\right)^e \left(\frac{\mu_\infty}{p_\infty v_\infty S^{1/2}}\right)^f. \quad (\text{A11})$$

Note that $\frac{\alpha_\infty}{V_\infty} = \frac{1}{M_\infty}$, where M_∞ is the free-stream Mach number. Also note that the dimensions of S are l^2 ; hence the dimension of $S^{1/2}$ is l , purely a length. Let

us choose this length to be the chord c by convention. Hence, $\frac{\mu_\infty}{\rho_\infty V_\infty S^{1/2}}$ can be replaced in our consideration by the equivalent quantity

$$\frac{\mu_\infty}{\rho_\infty V_\infty c} \rho_\infty V_\infty c. \quad (\text{A12})$$

However, $\frac{\mu_\infty}{\rho_\infty V_\infty c} \equiv \frac{1}{Re}$, where Re is based on the chord length c . Equation (A.11) thus becomes:

$$L = Z p_\infty V_\infty^2 S \left(\frac{1}{M_\infty} \right)^e \left(\frac{1}{Re} \right)^f. \quad (\text{A13})$$

We now define a new quantity, called the lift coefficient c_l , as:

$$\frac{c_l}{2} = Z \left(\frac{1}{M_\infty} \right)^e \left(\frac{1}{Re} \right)^f \quad (\text{A14})$$

Then Equation (A.13) becomes:

$$L = \frac{1}{2} \rho_\infty V_\infty^2 S c_l \quad (\text{A15})$$

Recalling from Chapter 4 that the dynamic pressure is $q = \frac{1}{2} \rho_\infty V_\infty^2$, we transform Equation (A.15) into:

$$L = q_\infty \cdot S \cdot c_l. \quad (\text{A16})$$

...Performing a similar dimensional analysis on drag and moments, beginning with relations analogous to Equation (A.1), we find that:

$$D = q_\infty S c_d. \quad (\text{A17})$$

Note: All derivation work done in Appendix A was not our own work, all credit goes to John Anderson, the author of “Introduction to Flight” textbook.

- [1] Galiński, C. et al. (2019) *Design and Investigation of Flat-Upper-Surface Airfoil*, ProQuest. Available at: [http://edmonds.idm.oclc.org/login?url=https%3A%2F%2Fwww.proquest.com%2Fscholarly-journals%2Fconstructual-theory-aeroelastic-design-flexible%2Fdocview%2F1952104376%2Fse-2%3Faccountid](http://edmonds.idm.oclc.org/login?url=https%3A%2F%2Fwww.proquest.com%2Fconference-papers-proceedings%2Fdesign-investigation-flat-upper-surface-airfoil%2Fdocview%2F2442612941%2Fse-2%3Faccountid) (Accessed: 29 November 2023).
- [2] Mardanpour, P. and Rastkar, S. (2017) *Constructal Theory and Aeroelastic Design of Flexible Flying Wing Aircraft*, ProQuest. Available at: <http://edmonds.idm.oclc.org/login?url=https%3A%2F%2Fwww.proquest.com%2Fscholarly-journals%2Fconstructual-theory-aeroelastic-design-flexible%2Fdocview%2F1952104376%2Fse-2%3Faccountid> (Accessed: 29 November 2023).
- [3] Abrams, M. (2022) *FOR SHEETS IN THE WIND: A close look at how paper airplanes fly (and fall) provides a new angle on aerodynamics*, *Mechanical Engineering*, 144(5), p. 64. Available at: <https://search-ebscohost-com.edmonds.idm.oclc.org/login.aspx?direct=true&db=aph&AN=158191473&site=ehost-live> (Accessed: 29 November 2023).
- [4] Huntley, I. (2000) *Flying - what you can find out with just a little bit of maths*, *Teaching Mathematics & its Applications*, 19(3), pp. 119–124. doi:10.1093/teamat/19.3.119. Available at: <https://search-ebscohost-com.edmonds.idm.oclc.org/login.aspx?direct=true&db=ehh&AN=44405646&site=ehost-live> (Accessed: 29 November 2023).
- [5] Li, H. et al. (2022) *Centre of mass location, flight modes, stability and dynamic modelling of gliders: Journal of Fluid Mechanics*, Cambridge Core. Available at: <https://bit.ly/3H42KdG> (Accessed: 29 November 2023).
- [6] Aerodynamics Explained by a World Record Paper Airplane Designer — Level Up — WIRED (2020), YouTube.
- [7] Newton's laws of Motion (2023), NASA. Available at: <https://www1.grc.nasa.gov/beginners-guide-to-aeronautics/newtons-laws-of-motion/#:~:text=Newtons%20first%20law%20states%20that,states%20of%20motion%20is%20inertia> (Accessed: 29 November 2023).
- [8] Coanda Effect, Available at: <http://www.thermofluids.co.uk/effect.php> (Accessed: 29 November 2023).
- [9] Bernoulli's principle, SKYbrary Aviation Safety. Available at: <https://skybrary.aero/articles/bernoullis-principle> (Accessed: 29 November 2023).
- [10] Kumar, A. (2023) Understanding stability in aircraft design, *Aviation*. Available at: <https://aviation.advancedtechworld.in/2023/03/understanding-stability-in-aircraft.html> (Accessed: 03 December 2023).
- [11] J. D. Anderson, *Introduction to Flight* (MCGRaw-HILL, S.l., MD, 2016).
- [12] Aerospace Engineering, D. of (2022) NACA 0024 - NACA 0024 airfoil, NACA 0024 (NACA0024-IL). Available at: <http://airfoiltools.com/airfoil/details?airfoil=naca0024-il> (Accessed: 03 March 2024).
- [13] Kraemer, A.S. (2020) ‘Naca airfoil 0012’ 3D models to print, yeggi. Available at: <https://www.yeggi.com/q/naca+airfoil+0012/> (Accessed: 03 March 2024).
- [14] Wurst, S. (2019) NIH 3D - NACA airfoils for wind tunnel testing, National Institutes of Health. Available at: <https://3d.nih.gov/entries/3dpx-012442> (Accessed: 03 March 2024).